Proceedings of the Seventeenth International Conference on
Civil, Structural and Environmental Engineering Computing
Edited by: P. Iványi, J. Kruis and B.H.V. Topping
Civil-Comp Conferences, Volume 6, Paper 7.2
Civil-Comp Press, Edinburgh, United Kingdom, 2023
doi: 10.4203/ccc.6.7.2

Calibration of beam bound model for the discrete element method

R. Varga and M. Čermák

Department of Mathematics
Faculty of Civil Engineering
VSB-TUO, Czech Republic

Abstract

The discrete element method (DEM) is a numerical method based on the motion and contacts of individual elements. It is mainly used in particle mechanics, because its possibilities of use for continuous problems are overshadowed by other methods, such as the finite element method (FEM). However, its application can be found, for example, in the problem of the size and propagation of cracks in concrete and reinforced concrete structures. These problems combine problems of continuous and particulate behavior, which causes problems in the calculations and optimization of commonly used FEM due to frequent changes in the mesh or the need for parameters that are difficult to detect in common practice. By using DEM, these problems are eliminated, but there is a need to properly define the properties of the solid bonded contacts, which are not found in the conventional DEM. This can be achieved using a variety of methods, this paper is focused on method that insert beams element between each particles called beam bound model (BBM).

Keywords: discrete element method, beam bound model, static and dynamics analysis

1 Introduction

The discrete element method is a numerical method for the analysis of discontinuous mechanics problems. It is based on the motion and interaction of uniform elements through contact. Its first theoretical foundations were laid in 1971 by P.A. Cundall in his paper [1]. In 1979 Cundall produced the first paper [2] mentioning the DEM. The method was subsequently extended in other papers, for example in a paper by J.R. Williams [3]. Over time, it has become a very powerful tool in dealing with particulate but also continuous materials that can be replaced by particulate systems, for example, its use for soils (A. Anandarajah [4]), rocks (L. Jing [5]), concrete (S. Hentz [6]), but also steel (A. Mohebkhah [7]).

Elements in DEM can be of any shape, general shapes are discussed in the paper by G. Lu [8], but for contact detection algorithms, circular and spherical elements are the most preferable, the advantages are discussed by J.P. Plassiard in [9]. Another important division is by contact type. There are two approaches to elements' behavior during contact, soft and hard contacts. The hard contacts do not allow the elements to penetrate each other, these elements are described by Stratton in paper [10]. Soft contacts allow mutual penetration, and the contact can take several time steps. This allows us to analyze changes in force transfer in the material but also allows us to use the interpenetration of the elements to preserve the deformability of the material. This type of contact is discussed in detail, for example, in the paper by Schwartz [11]. This paper will consider spherical elements with soft contacts.

2 Discrete element method – beam bound model

This section describes the basic principle of the DEM with an extension of BBM.

2.1 Equation of motion

Particle motion is based on the standard differential equation of motion of a rigid body with the following equation,

$$m\ddot{u} + c\dot{u} + ku = F_e, \tag{1}$$

where m – particle mass, c – damping, k – stiffness, u – displacement, F_e – external forces.

To solve (1), we use explicit time integration scheme described in Rojek [12]. We use the acceleration of the elements from the previous time step to calculate the internal contact and damping forces, which allows us to calculate the acceleration in the current time step,

$$\dot{u}^{(t+\Delta t)} = \dot{u}^{(t)} + \Delta t \ddot{u}^{(t)}, \tag{2}$$

$$u^{(t+\Delta t)} = u^{(t)} + \Delta t \dot{u}^{(t)} + \frac{1}{2}\Delta t^2 \ddot{u}^{(t)}, \tag{3}$$

$$\ddot{u}^{(t+\Delta t)} = -\frac{F}{m}, \tag{4}$$

where F is a sum of all forces applied to the element (Damping, Contact, External)

$$F = \sum (F_c + F_d \ + F_e), \tag{5}$$

where Δt – time step, F_c – contact forces, F_d – damping forces, F_e – external forces.

2.2 Contact and damping forces

We divide contacts into unbound and bonded. Unbounded contacts transmit only compressive and shear forces. The forces between the elements depend on the mutual penetration and relative motion of the elements. In our case, we consider the Hertzian model of contact between two parallel cylindrical bodies described in [13]. This type of contact occurs after the formation of cracks, so it is not considered in this paper.

The bonded contacts also allow the transmission of tensile forces and force moments. In method using BBM described in [14], fictive bar member is introduced between the discrete elements (Fig.1). This member is loaded with deformations depending on the mutual displacement of the elements. The end forces of the beam member are then applied as contact forces between the discrete elements. To calculate the end forces, we use a stiffness matrix obtained by the FEM described in [16],

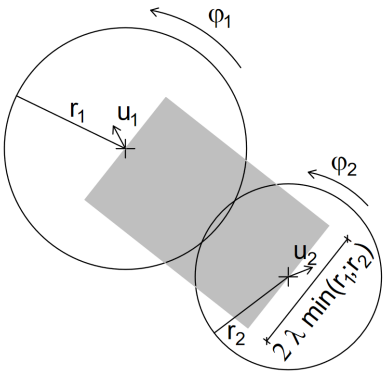

Figure 1: Bounded contact scheme

The stiffness matrix is defined as

$$K = \begin{bmatrix} \frac{AE}{l} & 0 & 0 & -\frac{AE}{l} & 0 & 0 \\ 0 & \frac{12EI}{l^3} & -\frac{6EI}{l^2} & 0 & -\frac{12EI}{l^3} & -\frac{6EI}{l^2} \\ 0 & -\frac{6EI}{l^2} & \frac{4EI}{l} & 0 & \frac{6EI}{l^2} & -\frac{2EI}{l} \\ -\frac{AE}{l} & 0 & 0 & \frac{AE}{l} & 0 & 0 \\ 0 & -\frac{12EI}{l^3} & \frac{6EI}{l^2} & 0 & \frac{12EI}{l^3} & \frac{6EI}{l^2} \\ 0 & -\frac{6EI}{l^2} & -\frac{2EI}{l} & 0 & \frac{6EI}{l^2} & \frac{4EI}{l} \end{bmatrix}, \tag{6}$$

$$h = 2\lambda \min(r_1, r_2),$$

$$A = bh \qquad I = \frac{1}{12} bh^3,$$

where I – beam cross-section moment of inertia, A – beam cross-section area, l – beam length, E – beam Young's modulus, h – beam height, b – beam thickness, λ – height coefficient.

The λ coefficient needs to be calibrated according to the type of task. A recommended value according to [14] is usually 0.7, but in cases of very dense grids with very variable element sizes, a much lower value may be preferable.

The Rayleigh damping matrix is used to calculate the damping forces. Its definition is given in [17], the final form of the matrix can be found in [14].

2.3 Contact and element stress

The stresses are divided into two categories, the first category is the BBM stresses where we find the maximum stress in a bounded contact. This stress is then compared to the maximum allowable stress within the bond, if the stress exceeds the connection is broken and a crack is formed. Stress is calculated as

$$\sigma_{max/min} = \frac{N}{A} \pm \frac{Mh}{2I} \tag{7}$$

$$\tau_{max} = \frac{3V}{2A} \tag{8}$$

where N – normal force, V – sheer force, M – bending moment, σ – normal stress, τ – sheer stress

The second is the stress on discrete elements. This stress is the output value of the analysis. It can be used as a value for design, but it is also considered necessary for the eventual calculation of crack widths and to express the actual deformation of the elements. The stress on the elements is expressed as the average stress of the whole element. The calculation procedure is given in [15] by the equations

$$\overline{\sigma}_p = \frac{1}{V_p} \int_{V_p} \sigma_p \, dV, \tag{9}$$

$\overline{\sigma}_p$ – average stress on element V_p – element volume

Since we do not consider the action of internal forces in the elements, and we also consider a finite number of element contacts, the equation can be modified to the form

$$\overline{\sigma}_p = \frac{1}{V_p} \sum_{n=1}^{n_c} F_c s_c \tag{10}$$

where s_c is vector from element center to the contact region.

3 Calibration of λ coefficient

According to F. Camborde in [18], the coefficient found in the axial test is also valid for more complex models using a similar mesh and element size.

In our case, the meshes of models used for calibration are set as shown below in Fig. 3. Tested beam is axially loaded by force of $F = 15$ MN, the cross-section of the beam is square with a side of 1 m. Young's modulus $E = 30$ GPa and Poisson's ratio $\nu = 0.25$. Tested value of $\lambda = \{1.00; 0.85; 0.70; 0.50\}$. Results are compared with an analytical solution.

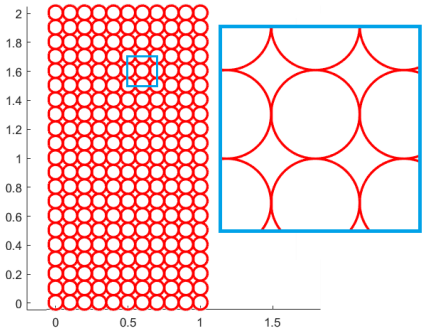

(a) Mesh type 1

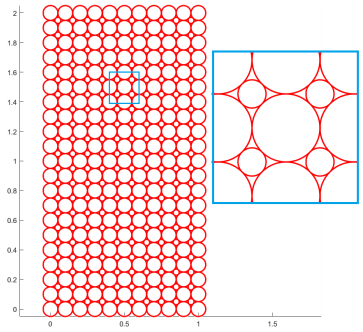

(b) Mesh type 2

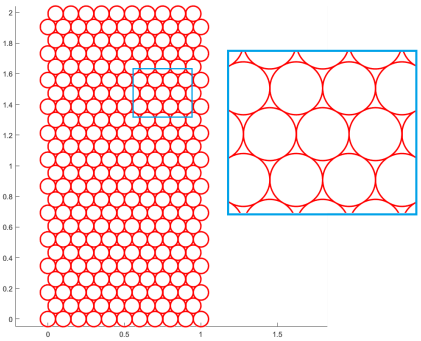

(c) Mesh type 3

Figure 2: Possibilities of beam discretization by circular DEM mesh.

Analytic solution of that problem is given by equation

$$d_{y,a} = \frac{Fl}{AE} = 1mm. \tag{11}$$

λ	Deformation d_y	$\frac{d_y}{d_{ya}}$
Mesh 1	mm	%
1.00	0.909	90.9
0.85	1.069	106.9
0.70	1.298	129.8
0.50	1.818	181.8

(a) mesh type 1

λ	Deformation d_y	$\frac{d_y}{d_{ya}}$
Mesh 2	mm	%
1.00	0.689	68.9
0.85	0.830	83.0
0.70	1.029	102.9
0.50	1.474	147.4

(b) mesh type 2

λ	Deformation d_y	$\frac{d_y}{d_{ya}}$
Mesh 3	mm	%
1.00	0.575	57.5
0.85	0.731	73.1
0.70	0.963	96.3
0.50	1.497	149.7

(c) mesh type 3

Table 1: Deformation based on λ coefficient

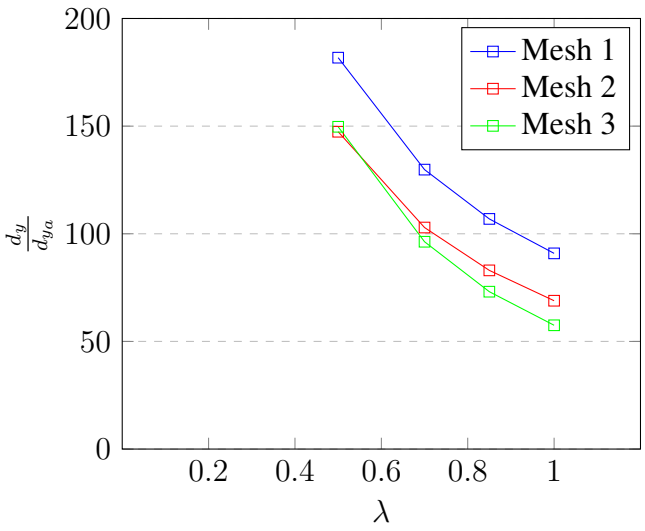

Figure 3: Relative deformation difference as a function of the λ coefficient

A power function is used to approximate the dependence of the deformation ratio on the lambda coefficient represented by Tab.1 and Fig.3. Using these functions, we

can find the most appropriate lambda coefficient for further calculations while maintaining a similar type of mesh.

$$\frac{d_y}{d_{y_a}} = a\lambda^b \tag{12}$$

For each type of mesh, using the least squares method, we obtain the coefficients for (12) and also the reliability value R^2.

Mesh	a	b	R^2	$(\frac{d_y}{d_{y_a}})_{(\lambda)} = 1$
1	0.9088	-1.000	1.0000	0.9088
2	0.6925	-1.095	0.9998	0.7149
3	0.5813	-1.377	0.9993	0.6743

Table 2: Coefficient of approximation equation

To prove theory from F. Camborde mentioned at beginning of this section, we going to analyse fixed beam using mesh type 2 with approximated λ as 0.715, see Tab.2. Results going to be compared with FEM solution by software ANSYS [19].

4 Fixed beam model

The problem to be solved is a bilaterally fixed beam with a length of 6 m loaded by a continuous load of 250 kN/m (Fig.4). The beam has a square cross-section with an edge length of 1 m and is made of a material with properties $E = 30$ GPa and $v = 0.25$. A mesh type 2 with coefficient $\lambda = 0.715$ is used for discretization.

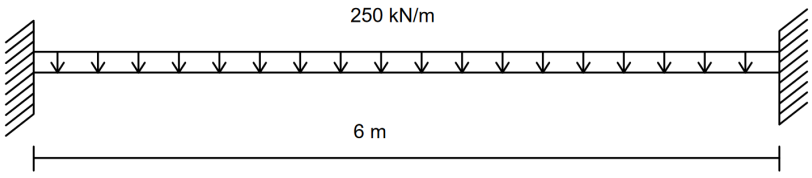

Figure 4: Fixed beam scheme

FEM/DEM	Source	Unit	Value	$\frac{DEM}{FEM}$ %
FEM DEM	$u_{y,max}$	mm	0.455 0.459	100.8
FEM DEM	$\sigma_{x,max}$	MPa	4.395 4.451	101.3
FEM DEM	$\sigma_{x,min}$	MPa	-4.336 -4.300	99.2
FEM DEM	$\tau_{xy,abs}$	MPa	1.101 0.948	116.1

Table 3: Result comparison DEM/FEM

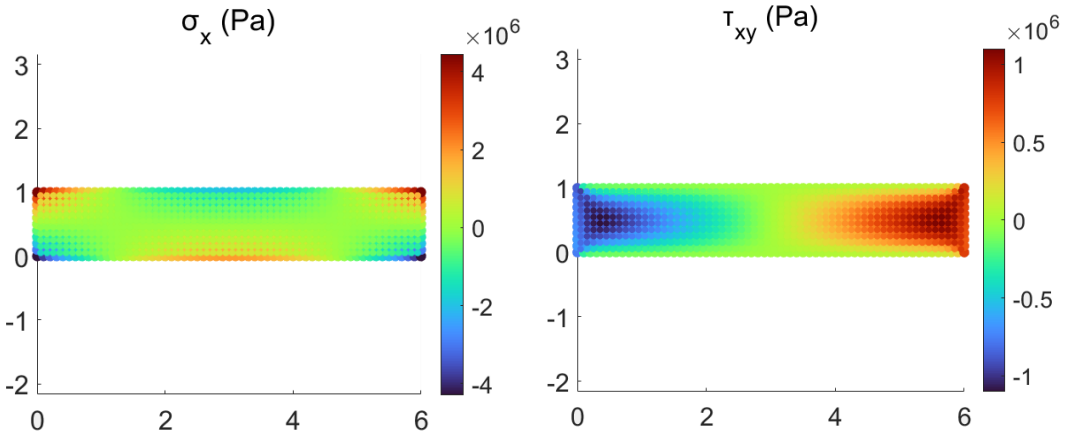

Figure 5: Mean stress in elements for DEM analysis

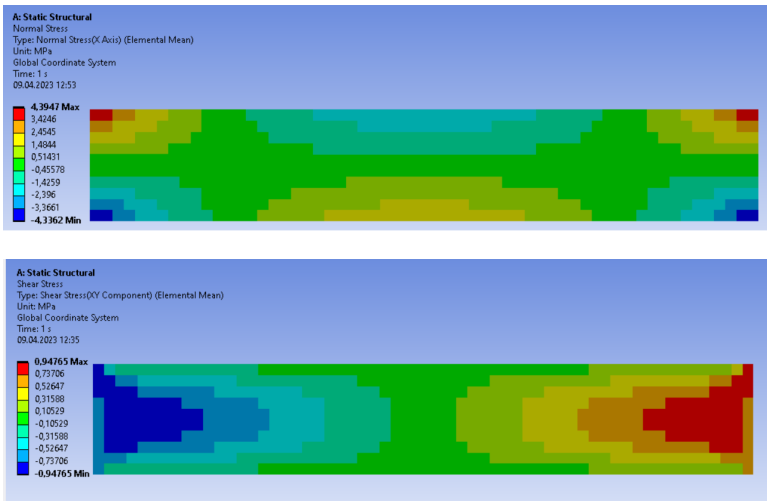

Figure 6: Mean stress in elements for FEM analysis

According to the results and comparison in Tab.3 and Fig.5,6 we can say that the above assumption can be applied in terms of deformation. Due to the use of different types of elements, the stresses cannot be directly compared. However, since despite these problems the error between the methods is in the order of units of percentage points and the stress values and stress flow are within the expected limits, the results can be considered acceptable.

5 Concluding remarks

The objective was to provide an overview and validation of the DEM-BBM method for further extension and research into the possibility of practical application of the method in the field of structural analysis, especially crack propagation in reinforced concrete structures.

Acknowledgements

The work was supported by the Student Grant Contest of VŠB-TUO. The project registration number is SP2023/021.

References

[1] P.A. Cundall. A Computer Model for Simulating Progressive Large Scale Movements in Blocky Rock Systems. *In Proc. Int. Symp. Rock Fracture*, ISRM, pages 2–8, Nancy, France, 1971.

[2] P.A. Cundall. Distinct element models of rock and soil structure. Analytical and computational models in engineering and rock mechanics. Allen&Unwin, London, 1987.

[3] J.R. Williams, G. Hocking, and G.G.W. Mustoe. The theoretical basis of the discrete element method. In NUMETA 1985, *Numerical Methods of Engineering, Theory and Applications*. A.A. Balkema, Rotterdam, 1985.

[4] A. Anandarajah. Discrete-element method for simulating the behavior of cohesive soil. *Journal of Geotechnical Engineering*, 1994, 120.9: 1593-1613.

[5] L. Jing, and O. Stephansson. Fundamentals of discrete element methods for rock engineering: *theory and applications*. Elsevier, 2007.

[6] S. Hentz, L. Daudeville, and F. V. Donzé. "Identification and validation of a discrete element model for concrete." *Journal of engineering mechanics* 130.6 (2004): 709-719.

[7] A. Mohebkhah , A. A. Tasnimi, and H. A. Moghadam. "Nonlinear analysis of masonry-infilled steel frames with openings using discrete element method." *Journal of constructional steel research* 64.12 (2008): 1463-1472.

[8] G. Lu, J. R. Third, and C. R. Müller. "Discrete element models for non-spherical particle systems: From theoretical developments to applications." *Chemical Engineering Science* 127 (2015): 425-465.

[9] J.P. Plassiard, N. Belheine, and F. V. Donzé. "A spherical discrete element model: calibration procedure and incremental response." *Granular Matter* 11.5 (2009): 293-306.

[10] R. E. Stratton, and C. M. Wensrich. "Modelling of multiple intra-time step collisions in the hard-sphere discrete element method." *Powder technology* 199.2 (2010): 120-130.

[11] S. R.Schwartz, D. C. Richardson, and P. Michel. "An implementation of the soft-sphere discrete element method in a high-performance parallel gravity treecode." *Granular Matter* 14.3 (2012): 363-380.

[12] J. Rojek, Contact modeling in the discrete element method. *Contact Modeling for Solids and Particles*. Springer, Cham, 2018. 177-228.

[13] V. L. Popov, Contact Mechanics and Friction: Physical Principles and Applications. Springer 2010, ISBN 978-3-642-10802-0

[14] M. Obermay, K. Dressler, C. Vretoss and P. Eberhard . "A bonded-particle model for cemented sand." *Computers and Geotechnics* 49 (2013): 299-313.

[15] S. Luding Macroscopic stress from dynamic, rotating granular media. *AIP Conf Proc.* 2010;1227(1):208-213

[16] N. Ganesan, R.C. Engels, Hierarchical Bernoulli-Euler beam finite elements. *Computers & Structures* 43/2 (1992). 297-304

[17] G. P. Henri Structural Element: Stiffness, Mass, and Damping Matrices. *CEE 541. Structural Dynamics* Fall 2020

[18] F. Camborde, C. Mariotti, and F. V. Donzé. Numerical study of rock and concrete behaviour by discrete element modelling. *Computers and geotechnics* 27.4 (2000): 225-247. https://doi.org/10.1016/S0266-352X(00)00013-6

[19] ANSYS, Inc., Ansys mechanical [software], official webpage, http://www.ansys.com (2022), accessed: 2022-07-22.